JOURNAL OF SOLID STATE CHEMISTRY 37, 58–66 (1981)

A Kinetic Study of the Oxidation and Reduction of Praseodymium Oxides: $(1/7)\ Pr_7O_{12} + (1/7 - x/2)\ O_2 \rightleftarrows PrO_{2-x}$

HIDEAKI INABA,* SHENG H. LIN, AND LEROY EYRING

Department of Chemistry and Center for Solid State Science, Arizona State University, Tempe, Arizona 85281

Received December 20, 1979; in revised form June 9, 1980

Kinetic and thermodynamic studies between the ordered ι ($n = 7$ in Pr_nO_{2n-2}) and the disordered α (PrO_{2-x}) phases have been carried out as a function of oxygen pressure at 655, 675, 695, and 715°C using a sample of small single crystals.

The existence of a reproducible hysteresis loop, which depends on the temperature and pressure, having an inflection point around a composition $PrO_{1.75}$ is shown. The inflection point is interpreted as a phase of $n = 8$ in Pr_nO_{2n-2} (η) coherently intergrown with $n = 7$, 9, and 10, giving an average composition of $PrO_{1.75}$.

In order to interpret the kinetic data, various theoretical models were examined, for example, oxygen diffusion, a phase-boundary reaction control, or nucleation and growth. None of these models, however, is capable of correlating the experimental data. It was found that a plot of the reaction rate versus the ambient oxygen pressure extrapolates linearly to a finite pressure at zero rate, as was previously observed in the oxidation reaction between the ι and ζ phases of the same system. The model developed for the oxidation reaction between the ι and ζ phases has been modified by taking into account the intermediate phases around $PrO_{1.75}$, through which the reaction passes. The modified rate law has two reaction constants: the rate constant from the reactant transforming to the intermediate phase (k_1) and for the transformation from the intermediate to the product phase (k_2). The fit to the experimental curve is satisfactory for both the oxidation and reduction reaction. From the temperature dependence of the observed rate constants, the activation energy for the oxidation and reduction was determined to be 75.0 and 60.9 kcal/mole, respectively.

1. Introduction

The intermediate praseodymium oxides form a fluorite-related homologous series (R_nO_{2n-2}, $n = 4$, 7, (8), 9, 10, 11, 12, ∞) of phases with well-defined stoichiometries and ordered structures (*1, 2*). In addition, two nonstoichiometric phases of wide composition range, $PrO_{1.5+x}$ and PrO_{2-x}, are observed at high temperatures (*3, 4*). Thermodynamic studies of phase transformations between these intermediate phases have shown that reproducible hysteresis loops are found when the phase reaction cycle is completed between any two phases (*3–12*). The causes of chemical hysteresis are no doubt varied and are not well understood in spite of its frequent occurrence in chemical systems. In order to understand the nature and the mechanism of hysteresis in any particular system, it is necessary to have a detailed knowledge of the structural, thermodynamic, and kinetic relationships of the phase reaction and to relate them

* On leave from the Department of Nuclear Engineering, Faculty of Engineering, Nagoya University, Nagoya, Japan.

0022-4596/81/040058-09$02.00/0

theoretically. In a paper on calorimetry (*12*), coherent intergrowth of many ordered phases between the ordered ι phase and the disordered α phase is considered responsible for the observed asymmetric hysteresis which is discussed in terms of the regular solution model (*10*). In a previous kinetic paper (*11*), it was found that for the kinetic reaction between ι ($n = 7$) and ζ ($n = 9$), none of the existing theoretical models (for example, those assumed to depend on diffusion, a moving boundary, a phase-boundary reaction control, nucleation and growth, etc.) is capable of correlating the experimental data. It was found that the rate of reaction is first order with respect both to the concentration of reactant and the ambient oxygen pressure. A linear plot of the reaction rate versus the ambient pressure yields a finite pressure at zero rate. This value extrapolated to zero rate corresponds to the lowest pressure of the product ζ phase along the oxidation path of the hysteresis loop. Due to the limitation of achievable experimental conditions, the reduction reaction between ι and ζ could not be studied in the previous work.

In the present kinetic study, both the oxidation and reduction reactions between the ordered ι phase and the disordered α phase are carried out. The kinetic behavior in this case is not as simple as that for the ι–ζ reaction due to the existence of the ordered intermediate phases between ι and α.

2. Experimental

Kinetic and thermodynamic measurements of the phase reaction

$$\frac{1}{7}\,Pr_7O_{12} + \left(\frac{1}{7} - \frac{x}{2}\right) O_2 \rightleftarrows PrO_{2-x} \quad (1)$$

have been carried out on specimens consisting of small single crystals using a Cahn RG thermobalance. The details of the experimental procedure were described in a previous paper (*11*).

Praseodymium oxide powder of 99.999% purity with respect to other rare earths was supplied by the Research Chemical Division of Nucor Corporation. The crystals were grown by a hydrothermal method (*13*), crushed and sized with Tyler series sieves to obtain a specimen weighing 314.55 mg with crystals ranging from 10 to 40 μm in diameter. The specimen was placed in a platinum basket 1.0 cm high and 0.6 cm in diameter. The irreproducibility and inaccuracy of the measurements were about ± 5 μg and ± 20 μg, respectively, corresponding to a compositional uncertainty of ± 0.0007 in the oxygen/metal ratio. The system was calibrated to determine the effect of thermal molecular flow (TMF) as a function of pressure at the experimental temperatures, using oxygen without the sample and argon with it. The largest TMF correction made in the data analysis was about 0.4 mg.

In the thermodynamic (hysteresis) study, the sample was kept at the desired temperature and a reduced pressure (as low as 5 Torr) for more than 5 hr to insure the production of the ι phase. Oxygen was then admitted and the weight change observed until equilibrium was attained. This process required a rather short time (from 10 to 30 min) in the single-phase regions, but a relatively long time (from 1 to 4 hr) in the two-phase regions.

In the kinetic runs in oxidation, the sample was kept at around 5 Torr at the desired experimental temperature for more than 3 hr to insure complete reduction to the ι phase. The pressure in the reaction chamber was finally adjusted to 10 Torr at the desired experimental temperature and the system allowed to attain equilibrium. The desired reaction pressure was obtained by opening a valve to a ballast where the oxygen pressure was higher than that in the reaction chamber. The temperature, pres-

sure, and weight were measured 1000 times consecutively in 0.5- to 4.0-sec intervals using an on-line PDP-8 computer. The final values were taken 1 to 8 hr later when the reaction was complete.

3. Results and Discussion

3.1 The Hysteresis Study

An isothermal hysteresis study has been carried out between the ι and α phases at different fixed temperatures by changing the pressure.

The results are shown in Figs. 1a–d. The compositions of the praseodymium oxides were not determined absolutely, rather the O/Pr ratio at the pressure of 10 Torr was assumed to be 1.714 on the basis of previous experience.

The features of the hysteresis curves are markedly different from those of the powder (*12*). The width of the hysteresis loop is small compared to that of the powder sample and there is an inflection point around an O/Pr ratio of 1.75. This confirms that the hysteresis loop depends on the crystal size (*9*). The inflection point near the O/Pr ratio 1.75 suggests the formation of a "phase" whose composition approaches that of $n = 8$ in Pr_nO_{2n-2} (η phase). A pure η phase has never been detected thermodynamically and almost never in the electron microscope, and since it does not have a stable pressure zone like ι or ζ, the "phase" $n = 8$ (η) is probably present coherently intergrown with ι and ζ as well as some higher members of the homologous series. This behavior has been observed in a sample quenched from the inflection point of the hysteresis loop using high-resolution electron microscopy (*14*). The shape of the hysteresis curve including the inflection point is similar at different temperatures although it shifts to higher pressures with an increased width as the temperature is increased.

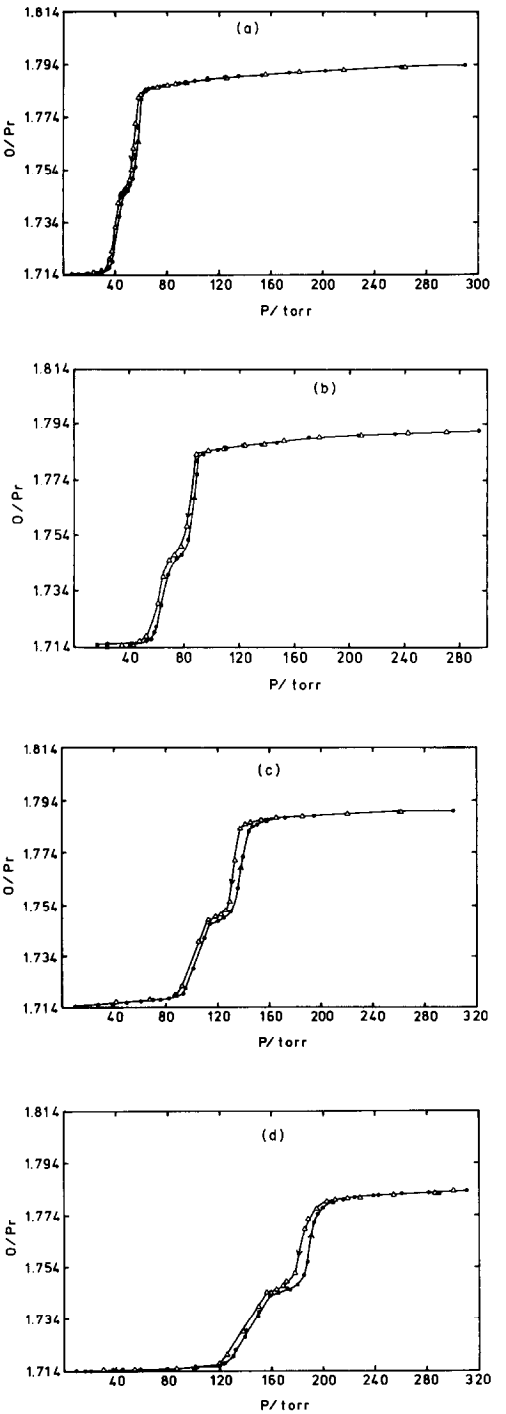

FIG. 1. Isothermal hysteresis loops between ι and α phases: (a) 655°C; (b) 675°C; (c) 695°C; (d) 715°C. •, Oxidation; △, reduction.

3.2 The Kinetic Study

A kinetic run at 675°C and a pressure of 99.4 Torr is shown plotted as a typical example in Fig. 2. Here the weight fraction, f, is plotted against the common logarithm of time, $\log t$. The weight fraction is

$$f = \frac{W - W_i}{W_f - W_i}, \qquad (2)$$

where W_f, W_i, and W are the final sample weight, initial sample weight and the sample weight at time t, respectively. As described in the experimental section, the pressure of the system initially kept at 10 Torr was suddenly increased to 99.4 Torr to start the phase reaction. The kinetic runs were made as a function of pressure at various temperatures. The pressure dependence of $1/t_{0.7}$ ($= U$) (the reciprocal of the time required for 70% reaction) is shown in Figs. 3a–d. As is apparent in this figure, U is linearly dependent on pressure.

Attempts to fit the measured kinetic curves to several theoretical models have been made. According to the diffusion model, the fractional weight change, f, for spherical particles is given by

$$f = 1 - \frac{6}{\pi^2} \sum_{n=1}^{\infty} \frac{1}{n^2} \exp(-n^2 D^* t), \qquad (3)$$

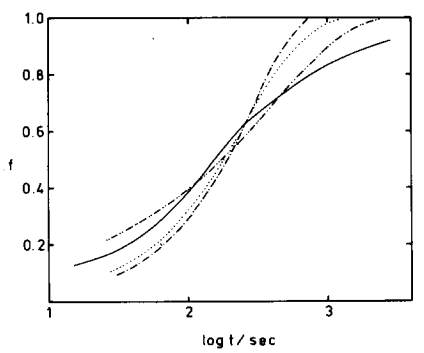

FIG. 2. A typical kinetic run at 675°C and 99.4 Torr and fitting of various models. The fraction of reaction is plotted against logarithm of time. ——, Observed curve; – · ·–, diffusion model; – · –, phase-boundary reaction model; · · · · ·, plate-like nucleation and growth model.

where $D^* = \pi^2 D/r_0^2$. D is the diffusion constant, and r_0 is the particle radius. Equation (3) is plotted to give the best fit to the experimental data in Fig. 2, but this model does not fit the experimental data well. Furthermore, the fact that the experimental kinetic curve does not fit Eq. (3) and the reaction rate, as illustrated in Fig. 3, is linearly dependent on pressure, suggests that the diffusion process is not rate determining.

The phase-boundary reaction model can be represented as

$$f = 1 - (1 - kt)^3, \qquad (4)$$

where k is the reaction constant. This model is also plotted in Fig. 2, but is seen not to fit the experimental data.

The plate-like nucleation and growth model can be expressed by

$$f = 1 - e^{-kt}, \qquad (5)$$

where k is the growth constant. It is also shown fitted to the data in Fig. 2, but the results are not encouraging.

In a previous paper (*11*), a new model was developed in which the oxidation reaction was assumed to pass through the oxidation branch of the hysteresis loop. Further, the reaction rate was first order with respect to both the concentration of phase A and the ambient pressure P. The rate equation was

$$-\frac{dA}{dt} = k'A(P - P_i), \qquad (6)$$

where k' is the rate constant, A the concentration of A and P_i the pressure of the intermediate phase along the oxidation branch of the hysteresis loop, as shown diagrammatically in Fig. 4. The resulting time dependence of f can be represented by

$$\frac{\beta(1 - f)}{\beta - f} = \exp[-k'(P - P_n)t], \qquad (7)$$

where $\beta = (P - P_0)/(P_n - P_0)$; P_0 and P_n are the beginning and the ending pressures

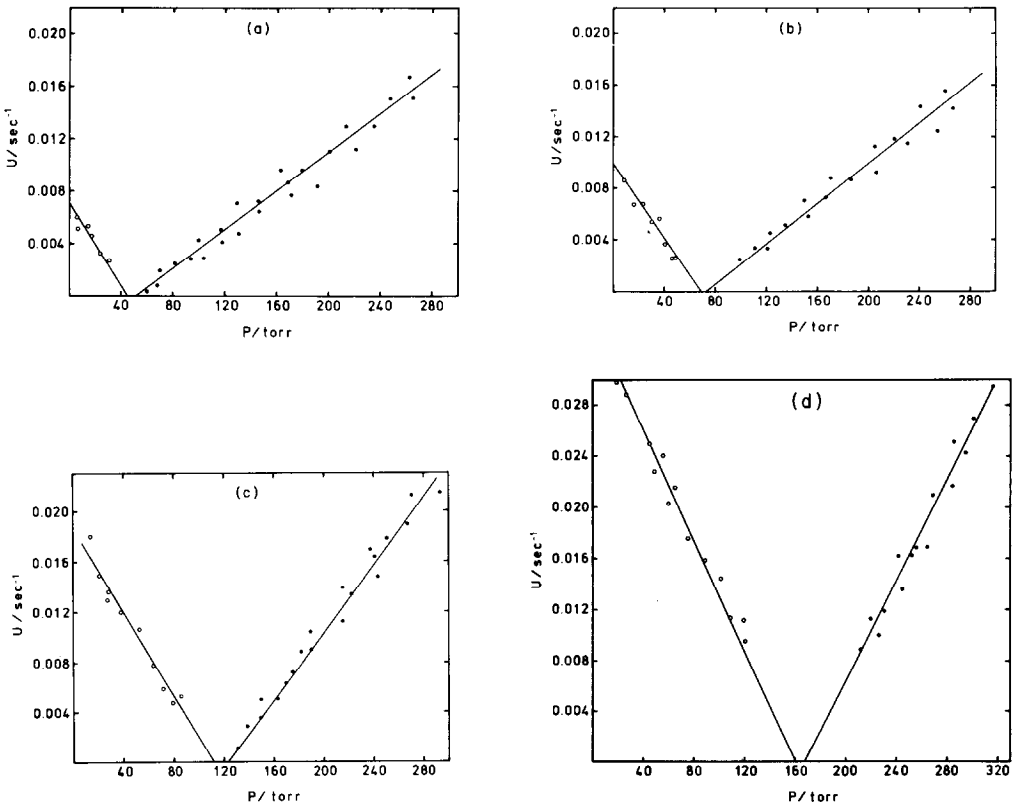

FIG. 3. U (the reciprocal of the time required for 70% reaction) against pressure. (a) 655°C; (b) 675°C; (c) 695°C; (d) 715°C. •, Oxidation; ○, reduction; ——, the theoretical calculations according to Eqs. (32) and (33).

of the oxidation branch of the hysteresis loop, respectively (Fig. 4). Equation 7 is plotted in Fig. 5, where β is taken as 1.21, which corresponds to P = 99.4 Torr at 675°C. As can be seen from Fig. 5, fitting of the experimental curve is still unsatisfactory.

The failure of any reasonable previous

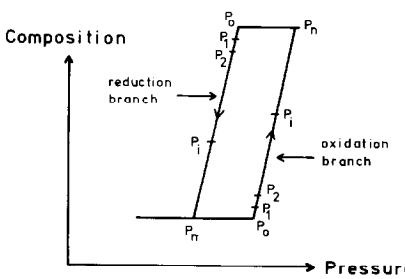

FIG. 4. An idealized isothermal hysteresis loop. Equilibrium pressures are marked for both oxidation and reduction paths.

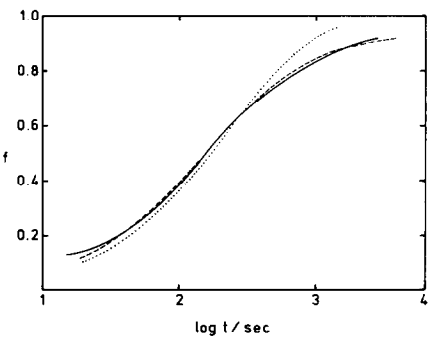

FIG. 5. Experimental and theoretical fits of f vs log t at 675°C and 99.4 Torr. ——, experimental curve, · · · · ·, calculated from Eq. (7), β = 1.21; – – –, calculated from Eq. (22); β = 1.21, K = 0.3.

model to apply to this reaction requires development of yet another model. In the hysteresis curves shown in Fig. 1 an inflection point occurs around $PrO_{1.75}$ between the ι and α phase. At this composition the system may consist mainly of an η phase ($n = 8$) coherently intergrown with ι, ζ, and ϵ ($n = 7$, 9, and 10 in Pr_nO_{2n-2}). Because of this "intermediate" phase, the kinetic behavior between ι and α is not as simple as that between ι and ζ, although the main features may still be the same. The model previously developed (*11*) can be modified taking into account the "intermediate" phases occurring in the course of the reaction. For the oxidation reaction we take the original ι phase, the intermediate phase, and the final α phase as A, B, and C, respectively. The whole reaction can then be represented as:

$$A \xrightarrow[O_2]{k_1'} B \xrightarrow[O_2]{k_2'} C. \tag{8}$$

As assumed in the previous paper, the reaction passes through all the intermediate phases of the hysteresis curve, including in this case, the "intermediate" phase, B. Accordingly, we have two different reaction constants k_1' and k_2' as shown in Eq. (8). The rate equations for A, B, and C may then be written as

$$-\frac{dA}{dt} = k_1'A(P - P_i), \tag{9}$$

$$-\frac{dB}{dt} = k_2'B(P - P_i) - k_1'A(P - P_i), \tag{10}$$

$$\frac{dC}{dt} = k_2'B(P - P_i), \tag{11}$$

where A, B, and C are the concentrations of the reactants A and B and the product C, P is the ambient pressure and P_i is the equilibrium pressure of the intermediate states along the hysteresis curve shown in Fig. 4. The term $(P - P_i)$ in Eq. 9 means that the reaction does not proceed until the ambient pressure P reaches P_i, the equilibrium pressure of the intermediate states.

In order to convert this rate expression into one expressed in terms of weight fraction, f, we introduce the weight of the sample W.

$$W = V(AM_A + BM_B + CM_C), \tag{12}$$

where V is the volume of the sample, A, B, and C denote concentrations as before and M_A, M_B, and M_C represent the molecular weights of A, B, and C, respectively. At time zero and infinity, we have

$$W_0 = VA_0M_A \tag{13}$$

and

$$W_\infty = V(A_\infty M_A + B_\infty M_B + C_\infty M_C), \tag{14}$$

respectively. Here we assume for the sake of simplicity that the molecular weight of the "intermediate" phase is the average of the original and product phases; i.e.,

$$M_B = M/2 + M_A$$
$$M_C = M + M_A. \tag{15}$$

Using Eq. (15) and noticing that

$$A + B + C = A_\infty + B_\infty + C_\infty = A_0 \tag{16}$$

we obtain

$$f = \frac{W - W_0}{W_\infty - W_0} = \frac{\frac{1}{2}B + C}{\frac{1}{2}B_\infty + C_\infty}. \tag{17}$$

From Eqs. (9) and (10) we get

$$\frac{dB}{dA} = \frac{k_2'}{k_1'}\frac{B}{A} - 1. \tag{18}$$

Putting k_2'/k_1' as K and solving Eq. (18), we get

$$A^{-K}B = \frac{1}{K - 1}A^{1-K} + C_1, \tag{19}$$

where C_1 is the integration constant. We normalize A_0 to be 1 for simplicity and when $A = A_0 = 1$, B is zero, then $C_1 = 1/1 - K$ and

$$B = \frac{A - A^K}{K - 1}. \tag{20}$$

We have chosen the reaction pressure as $P > P_n$ so that $\frac{1}{2}B_\infty + C_\infty = C_\infty = A_0 = 1$. Equation (17) then becomes

$$f = \frac{B}{2} + C. \tag{21}$$

Using Eqs. (16), (20), and (21)

$$f = \frac{A^K - (2K - 1)A + 2(K - 1)}{2(K - 1)}. \tag{22}$$

Assuming that the oxidation path of the hysteresis is linear against pressure, as illustrated in Fig. 4,

$$P_i = P_0 + f(P_n - P_0). \tag{23}$$

Equation (9) then becomes

$$-\frac{dA}{dt} = k_1' A(\beta - f)\alpha, \tag{24}$$

where

$$\beta = \frac{P - P_0}{P_n - P_0} \tag{25}$$

and

$$\alpha = P_n - P_0. \tag{26}$$

Substituting Eq. (22) into Eq. (24), we get

$$-\frac{dA}{dt} = \frac{k_1'\alpha\{A^{K+1} - (2K - 1)A^2 + 2(1 - K)(\beta - 1)A\}}{2(1 - K)}. \tag{27}$$

By determining the integration range we obtain

$$-\int_1^A \frac{2(1 - K)dA}{\{A^{K+1} - (2K - 1)A^2 + 2(1 - K)(\beta - 1)A\}} = \int_0^t k_1'\alpha dt = k_1'\alpha t. \tag{28}$$

This integration can be performed numerically for different A and K by assigning a value to the parameter β, and putting it into $I(A, K)$;

$$I(A, K) = -\int_1^A \frac{2(1 - K)dA}{A^{K+1} - (2K - 1)A^2 + 2(1 - K)(\beta - 1)A}. \tag{29}$$

This integration can be performed numerically by assigning values to the parameters K and β. β is determined from the experimental pressure and the hysteresis curve of the same temperature shown in Fig. 1 using Eq. (25). K is the parameter which changes the shape of the kinetic curve and it is determined by fitting the experimental curve. Given both β and K, the integration can be performed to give $k_1'\alpha t$ for any value of A. A can be converted into f using Eq. (22) providing f as a function of $k_1'\alpha t$. The unknown reaction constant, k_1' can be determined by fitting the experimental kinetic curve by shifting it along $\log t$. An example of the calculation with $K = 0.3$, $\beta = 1.21$ and the fitting of the experimental result at 675°C and $P = 99.4$ ($\beta = 1.21$) is shown in Fig. 5. The fit is satisfactory. The time dependence of A, B, C, and f for $K = 0.3$ and $\beta = 1.21$ is shown in Fig. 6 where A is seen to decrease monotonically, C increases monotonically, and B increases at first and then decreases.

In order to compare observed values with those calculated, $I(A_{f=0.7}, K)$ was evaluated, where $A_{f=0.7}$ is the value A at $f = 0.7$

$$I(A_{f=0.7}, K) = (P_n - P_0)k_1' t_{0.7}. \tag{30}$$

Consider a free-energy level versus the

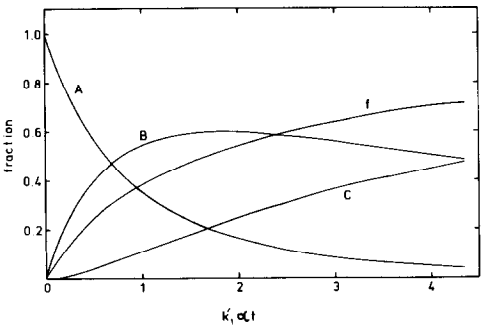

FIG. 6. The time dependence of A, B, C, and f for $K = 0.3$ and $\beta = 1.21$ calculated by using Eq. (29).

reaction-coordinate diagram, and notice that the initial free energy is dependent on P_0 because the phase reaction does not proceed until this pressure is reached. k_1' depends on the temperature through P_0 and the dependence of k' on P_0 can be taken into account by shifting the energy of the initial state by the amount, $RT \ln P_0$; i.e.,

$$k_1' = k_1 \exp \frac{(-RT \ln P_0)}{RT} = \frac{k_1}{P_0}. \quad (31)$$

Substituting Eq. (31) into Eq. (30), we get

$$1/t_{0.7} = \frac{P_n - P_0}{P_0} \frac{k_1}{I(A_{f=0.7}, K)}. \quad (32)$$

From Eq. (32), we can calculate $1/t_{0.7}$ by fitting k_1 to the experimental values at each temperature. In Fig. 3 the calculated values are shown as the solid line, where the value of K is scattered around the value listed in Table I at each temperature depending on the ambient pressure used in the kinetic curve fitting, but it is taken as that value for all β in that calculation. As can be seen in Fig. 3, the observed and calculated data are in good agreement. The value of K varied slightly depending on the reaction temperature as listed in Table I.

TABLE I

VALUE OF K AT VARIOUS TEMPERATURES

Temperature (°C)	Oxidation	Reduction
655	0.4	0.6
675	0.3	0.3
695	0.25	0.25
715	0.3	0.25

None of the existing models suggests a linear relationship between the reaction rate and the ambient pressure. The rate equation (Eqs. (9)–(11)) suggests that two atoms of oxygen are involved in the rate-determining step of the reaction. The linear extrapolation of the rate with pressure to zero rate correlates with the observed fact that the rate is zero below some finite pressure at any temperature. The extrapolations in both oxidation and reduction correspond to the equilibrium pressure of the β phase, as is apparent from Figs. 1 and 3.

In the reduction reaction the rate equation would be the same as the oxidation reaction if we take the concentration of the original α phase, intermediate phase, and the final ι phase as A, B, and C, respectively. Equations (9)–(31) hold also in this case when we put $\alpha = P_0 - P_n$ instead of $\alpha = P_n - P_0$, where P_0 is the lowest pressure in the α phase and P_n is the highest pressure in the ι phase along the reduction branch of the hysteresis loop. The quantity $1/t_{0.7}$ in the reduction reaction can be written as

$$1/t_{0.7} = \frac{P_0 - P_n}{P_0} \frac{k_1}{I(A_{f=0.7}, K)}. \quad (33)$$

The calculated values from Eq. (33) and the experimental data are shown in Fig. 3 for comparison. Good agreement is observed. The temperature dependence of K is shown in Table I. From Eqs. (32) and (33) the rate constant k_1 for both the oxidation and reduction reactions can be determined. Arrhenius plots of k_1 are shown in Fig. 7. Activation energies of 75.0 and 60.9 kcal/mole are obtained for the oxidation and reduction reactions, respectively. The activation energy for oxidation is 75.0 kcal/mole to be compared with 45.3 kcal/mole obtained for the activation energy for the oxidation of

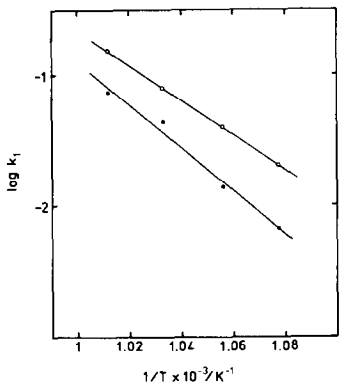

FIG. 7. A plot of $\log k_1$ against $1/T$ for the oxidation and reduction reactions. •, Oxidation; o, reduction.

the ι to the ζ phase (*11*). To give the reason for the higher activation energy in the present case would be difficult, since we do not know the exact rate-determining step of the reaction. However, if one assumes that the rate-determining step involves the movement of the oxygen-vacancy pair from its position in ι ($n = 7$) to that in ζ ($n = 9$) or η ($n = 8$, the present case), it would be observed that the movement from $n = 7$ to $n = 9$ would require less energy than that from $n = 7$ to $n = 8$, because odd members of the homologous series are structurally different from even ones (*1, 2*). The smaller activation energy for the reduction, 60.9 kcal/mole, suggests that in the α phase where the oxygen vacancies are randomly distributed they would be more easily nucleated into any ordered phase of $n = 7$, 8, 9, and 10 in Pr_nO_{2n-2}.

Acknowledgments

The National Science Foundation, under Grant DMR 78-05722, supported this work. The single crystals were prepared by Michael McKelvy. For all this support the authors express their appreciation.

References

1. P. KUNZMANN AND L. EYRING, *J. Solid State Chem.* **14,** 229 (1975).
2. R. T. TUENGE AND L. EYRING, *J. Solid State Chem.* **29,** 165 (1979).
3. B. G. HYDE, D. J. M. BEVAN, AND L. EYRING, *Philos. Trans. Roy. Soc. London Ser. A,* **259,** 583 (1966).
4. D. A. BURNHAM AND L. EYRING, *J. Phys. Chem.* **72,** 4415 (1968).
5. D. A. BURNHAM, L. EYRING, AND J. KORDIS, *J. Phys. Chem.* **72,** 4424 (1968).
6. J. KORDIS AND L. EYRING, *J. Phys. Chem.* **72,** 2044 (1968).
7. R. P. TURCOTTE, M. S. JENKINS, AND L. EYRING, *J. Solid State Chem.* **7,** 454 (1973).
8. A. T. LOWE AND L. EYRING, *J. Solid State Chem.* **14,** 383 (1975).
9. A. T. LOWE, K. H. LAU, AND L. EYRING, *J. Solid State Chem.* **15,** 9 (1975).
10. D. R. KNITTEL, S. P. PACK, S. H. LIN, AND L. EYRING, *J. Chem. Phys.* **67,** 134 (1977).
11. H. INABA, S. PACK, S. H. LIN, AND L. EYRING, *J. Solid State Chem.* **33,** 295 (1980).
12. H. INABA, A. NAVROTSKY, AND L. EYRING, *J. Solid State Chem.* **36,** 000 (1981).
13. J. M. HASCHKE AND L. EYRING, *Inorg. Chem.* **10,** 2267 (1971).
14. K. FORGHANY, H. INABA, AND L. EYRING, unpublished results.